IEEE Access
Multidisciplinary | Rapid Review | Open Access Journal

Received September 8, 2020, accepted September 18, 2020, date of publication September 23, 2020,
date of current version October 2, 2020.

Digital Object Identifier 10.1109/ACCESS.2020.3026037

Corticomuscular Co-Activation Based Hybrid Brain-Computer Interface for Motor Recovery Monitoring

ANIRBAN CHOWDHURY[1], ASHISH DUTTA[2], (Member, IEEE), AND GIRIJESH PRASAD[3], (Senior Member, IEEE)

[1]School of Computer Science and Electronic Engineering, University of Essex, Colchester CO4 3SQ, U.K.
[2]Department of Mechanical Engineering, Indian Institute of Technology Kanpur, Kanpur 208016, India
[3]Intelligent Systems Research Centre, Ulster University, Derry-Londonderry BT48 7JL, U.K.

Corresponding author: Anirban Chowdhury (a.chowdhury@essex.ac.uk)

This work was supported in part by the Department of Science and Technology, India, and in part by the U.K.—India Education and Research Initiative (UKIERI)—Thematic Partnership Project A BCI Operated Hand Exoskeleton-Based Neurorehabilitation System under Grant UKIERI-DST-2013-14/126, Grant DST/INT/UK/P-80/2014, and Grant DST-UKIERI-2016-17-0128.

ABSTRACT The effect of corticomuscular coactivation based hybrid brain-computer interface (h-BCI) on post-stroke neurorehabilitation has not been explored yet. A major challenge in this area is to find an appropriate corticomuscular feature which can not only drive an h-BCI but also serve as a biomarker for motor recovery monitoring. Our previous study established the feasibility of a new method of measuring corticomuscular co-activation called correlation of band-limited power time-courses (CBPT) of EEG and EMG signals, outperforming the traditional EEG-EMG coherence in terms of accurately controlling a robotic hand exoskeleton device by the stroke patients. In this paper, we have evaluated the neurophysiological significance of CBPT for motor recovery monitoring by conducting a 5-week long longitudinal pilot trial on 4 chronic hemiparetic stroke patients. Results show that the CBPT variations correlated significantly (p-value< 0.05) with the dynamic changes in motor outcome measures during the therapy for all the patients. As the bandpower based biomarkers are popular in literature, a comparison with such biomarkers has also been made to cross-verify whether the changes in CBPT are indeed neurophysiological. Thus the study concludes that CBPT can serve as a biomarker for motor recovery monitoring while serving as a corticomuscular co-activation feature for h-BCI based neurorehabilitation. Despite an observed significant positive change between pre- and post-intervention motor outcomes, the question of the clinical effectiveness of CBPT is subject to further controlled trial on a larger cohort.

INDEX TERMS Biomarkers, brain-computer interfaces, electroencephalography, electromyography, exoskeletons, neurofeedback, rehabilitation robotics, stroke.

I. INTRODUCTION

Introduced by Pfurtscheller and colleagues in 2010 the concept of hybrid-brain computer interfaces (h-BCI) is an active area of research in BCI. As per the definition, h-BCI exploits two different modalities of brain-wave or combines other physiological signals with brain signals in a simultaneous or sequential manner to enhance the performance of a conventional BCI [1]. The early development of h-BCI combining different brain signal modalities such as event-related desynchronization (ERD) and steady-state visually evoked potentials (SSVEP) in a simultaneous [2], [3] or sequential [4] way showed reduced false positive rate and enhanced accuracy. Notably, ERD is associated with a change in the rhythmic activity characterised by a localized and short-lasting decrease in the amplitude in alpha/beta frequency bands whereas an increase in amplitude is referred to as Event-related Synchronization (ERS) [5]. Other physiological signals such as eye-tracking and heart-rate (HR) are also combined sequentially with brain signals (ERD and SSVEP) where one of the modalities acted as a brain-switch for the next stage to reduce the error in decoding [1]. In an

The associate editor coordinating the review of this manuscript and approving it for publication was Yuan-Pin Lin.

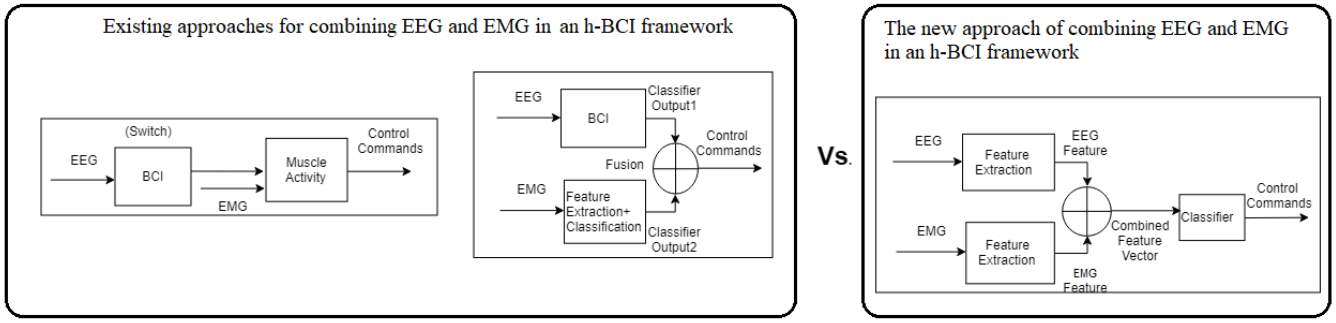

FIGURE 1. Comparison between existing approaches of combining EEG and EMG in an h-BCI framework with the new approach. The proposed new approach combines the EEG and EMG signals at the input stage to generate a hybrid feature that is shown on the right-hand side. The proposed approach is different from a similar approach where EEG and EMG features are combined after extracting them separately.

eye-tracking+ERD based h-BCI paradigm the dwell time based switching of a certain button on a computer screen can be replaced by an ERD-BCI based brain switch for better personalization, while the selection of the buttons can be made using the eye-tracking signals for increasing the number of commands [6]. It is well established that heart rate can be voluntarily modulated by the somatomotor process connected to mental activity. The combination of heart-rate modulation with SSVEP was used to control a prosthetic arm where the h-BCI system is switched on by the heart-rate modulation and then SSVEP was used to direct the prosthetic arm to execute various motions to achieve a particular task [7]. Different fusion techniques using EEG, EMG, and mechanomyogram (MMG) were also evaluated for multijoint lower-limb control with improved accuracy [8]. A controlled study on an h-BCI system composed of motor-imagery (MI) and selective sensation proved that it performed significantly better than the only MI-based BCI [9]. Control of multi-degree of freedom robotic arm is also proved to be possible using an h-BCI combining more than two signals [10]. Thus three major purposes of h-BCI is identified in the literature so far are enhancing classification accuracy, improving the number of control commands, and reducing the signal detection time [11].

The approach of combining EEG and EMG signals in an h-BCI framework presented in this paper is a bit different from the existing approaches which is illustrated in Fig. 1, where it can be seen that while the existing approaches to combine EEG and EMG hybridize the two systems (a BCI with another BCI or a different human-computer interface) at the output level, the h-BCI in this paper correlates the changes in a brain signal (EEG) with a physiological signal (EMG) at the input level and forms a single system as an h-BCI. In particular, we have correlated the EEG and EMG signals to engineer a new feature which is then used for the classification purposes [12]. This is different from calculating EEG and EMG features separately and then combining it in a single feature vector. For example, one can calculate the EEG bandpower features (BP) from different channels (say the dimension is m) and the mean absolute value (MAV) of EMG from different channels (say the dimension is n). Then combine the m dimensional BP feature from EEG and n dimensional MAV feature from EMG to create a single feature vector of dimension $m + n$. Rather than going by this approach, we calculated a single feature, called the correlation of band-limited power time-courses (CBPT) [12] for different EEG-EMG channel combinations. However, we do not argue that this is a different category of h-BCI architecture, rather it should only be considered as a different approach of feature vector formation using a novel EEG+EMG feature. It is worth mentioning that this approach of combining EEG and EMG is also different from combining (simultaneous or sequential) the outputs of EEG and EMG classifiers [13]. The reason behind designing a new architecture of h-BCI rather than going for the existing architectures lies in the quest for finding a metric for cortical and peripheral nerve connectivity which will be suitable not only for providing neurofeedback related to a therapeutic exercise but also effective for motor recovery monitoring. It has been found in the past that multimodal fusion between EEG and EMG activity leads to more reliable performance than EMG or EEG alone [13].

Corticomuscular coactivation has neurophysiological significance as it was found to be one of the underlying mechanisms for effective corticospinal interaction which can improve motor functionality [14]. Such coactivations are also distinguishable for individual finger motions in the case of stroke patients [15]. Strong corticomuscular coactivation was also observed at the contralateral motor cortex for both impaired and unimpaired hand, which can reflect motor functional recovery after stroke [16]. The connection between the cortex and muscle plays an important role in motor recovery as it is found in a recent study that corticomuscular coherence (CMC) acts as a potential biomarker for the quantification of motor deficit [17], [18]. Apart from hand, CMC can be observed in other body parts too, such as in tibialis anterior muscle in the lower leg during isometric contraction [19]. Voluntary change in motor behaviour can also modulate the strength of CMC within a neurofeedback paradigm for upper-limb activity [20]. An offline analysis of different finger motions of stroke patients using CMC also

revealed its utility for active rehabilitation [21]. However, CMC is not suitable for single-trial based prediction of motor activity. One of the major reasons for this is that the CMC is greatly reduced following stroke [17], [22] and also shows a dynamic shift in frequency due to fatigue [23]. It also suffers from estimation vs. resolution issues for shorter time segments (as in the case of single-trial based detection), lower signal-to-noise ratio, especially when lower muscle mass is involved in slow finger movements [12], [24]. Therefore, our previous work investigated the feasibility of a new corticomuscular coactivation index based on the correlation of the band-limited power time-courses (CBPT) between EEG and EMG [12]. EEG-EMG CBPT measures the corticomuscular coactivation in terms of changes in the EEG and EMG band power. It showed that an EEG-EMG CBPT based h-BCI system was able to perform significantly better than a CMC based h-BCI in providing hand-exoskeleton based neurofeedback to the stroke patients.

Although suitable for detecting attempted motor movement in a single trial [12], estimating the relation of EEG-EMG CBPT with motor recovery required a longitudinal clinical trial on stroke patients. Despite the potential of conventional BCI systems in controlling different neuroprotheses [25], virtual-reality [26] and orthotic devices [27], [28] has been extensively evaluated for the past few years, the evaluation of h-BCI devices in clinical perspective is much ignored. A recent study used the EEG and EMG signals in a sequential h-BCI architecture where EEG is used for movement initiation while EMG is used for finer control, estimating the joint angles [29]. Here the EEG-EMG based h-BCI was found feasible for real-time control by the stroke patients, however, they didn't study its relation with motor recovery. Moreover, the EEG and EMG were used as separate sub-systems connected sequentially and hence corticomuscular coactivation was not used for control which is important to be tested considering its importance from a rehabilitation point of view [30]. A recent study on movement-related cortical potential (MRCP) has also shown the utility of simultaneous activation of EEG and EMG signals as a comprehensive approach for neurofeedback training in action observation, motor imagery, and motor execution of sitting and standing tasks, which could lead towards the advancement of exoskeleton-based rehabilitation [31].

In order to meet this need, we present a preliminary study on chronic stroke patients wherein they have used the EEG-EMG CBPT based h-BCI system to get hand-exoskeleton based neurofeedback of their finger motions. The design of the experiment as a single-arm study aims at discovering the relationship of EEG-EMG CBPT with the motor outcome measures so that it can serve as a possible biomarker for motor recovery monitoring. During the 5-week-long study, we have monitored the motor-recovery outcome by standard measures such as Action-research-Arm-Test (ARAT) and grip-strength (GS) for pre, post, and every week during the therapy period. The relationship between the motor outcome and EEG-EMG CBPT is estimated to validate its use as a biomarker for recovery. As the estimation of a patient's motor recovery is a major prognostic challenge for the clinicians [32], comparison with popular bandpower based biomarker has also been made to cross-verify whether the changes in CBPT are indeed neurophysiological.

II. MATERIALS AND METHODS

A. ETHICS STATEMENT

The University Research Ethics Committee of the Ulster University approved the study protocol, which followed all the regulations and guidelines of the Declaration of Helsinki. The trial was retrospectively registered at the isrctn.com[1] (ISRCTN13139098). All the participants gave their consent by signing the informed consent form. All the data recorded during the trial are de-identified and stored anonymously.

B. PARTICIPANTS

The University Research Ethics Committee of the Ulster University approved the study protocol, which followed all the regulations and guidelines of the Declaration of Helsinki. All the participants gave their consent by signing the informed consent form. All the data recorded during the trial are de-identified and stored anonymously.

The post-stroke motor recovery generally plateaus after 3 months and the more time passes from the stroke incidence, the chances of auto-recovery and recovery by traditional means of therapy diminish. This is the point where alternative means of recovery can be tested. Therefore, we have recruited 5 chronic stroke (ischemic) patients suffering from hemiparesis. The mean time since the first occurrence of stroke was 21.8±4.49 within the range 17 to 28 months. As revealed by the testimonials of the patients, their motor functionality stopped improving for the last one year. These patients were selected out of 15 who were initially interviewed and then gradually filtered out by the inclusion/exclusion criteria and exoskeleton fitment test. Out of these 5 patients allocated for the intervention, 1 patient (S05 in Table 1) had an accidental hand-fracture (disconnected incident from the trial) and left the trial after 2 weeks. Finally, the rest of the 4 completed the trial and were analysed. The flow diagram from the recruitment to the analysis is depicted as per the CONSORT recommendation in Fig. 2. The patient demographics have been shown in Table 1. All the patients were recruited locally (2 males and 3 females) having an average age of 61.6±5.3 (range 56–69). Two of the participants had impairment in the left hand while 3 of them had their impairment in the right hand. All of them are reported to be right-handed. The baseline measurements of motor-functionality as measured by ARAT and GS were 24±10.88 and 10.7±4.4 kg respectively. All the patients had some sort of residual muscle activity as measured by EMG. The brain areas affected by lesion after

[1] https://doi.org/10.1186/ISRCTN13139098

TABLE 1. Baseline demographics of the participants.

Patient Code	Sex	Age (years)	MMSE (Total=30)	Affected Side	Months Since Stroke	ARAT (baseline)	ARAT (Final)	GS (kg) (baseline)	GS (kg) (Final)	Stroke Type	Location of Brain lesion
S01	F	60	28.5	Right	22	35	57	3	20	Ischemic	Left side of Pons
S02	M	56	30	Left	28	6	31	11.7	16.67	Ischemic	Right middle cerebral Artery
S03	F	69	28	Right	24	29	56	13.7	23	Ischemic	Left frontal lobe peri-ventricular and basal ganglia
S04	F	65	27	Left	18	24	45	12	20	Ischemic	Thalamus
S05	M	58	28	Right	17	26	-	13.3	-	Ischemic	Brain Stem

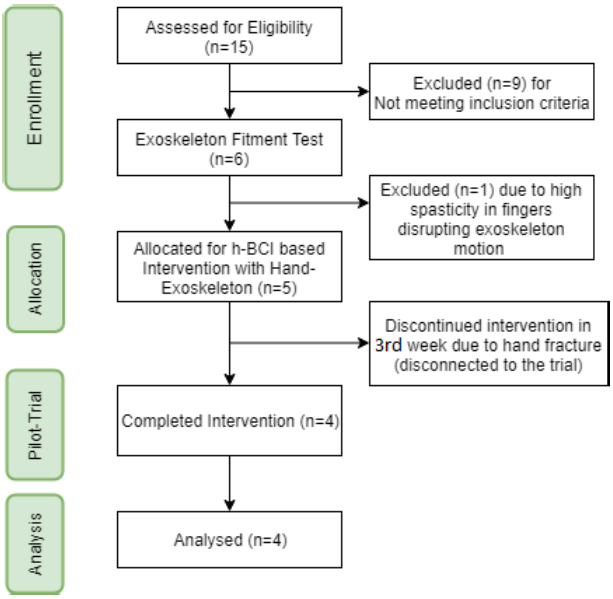

FIGURE 2. CONSORT Diagram. This shows in a systematic way how the trial has proceeded right from the recruitment to the analysis stage.

stroke as revealed by the Magnetic Resonance Imaging (MRI) reports are mentioned at the rightmost column of Table 1.

The inclusion criteria of the participants are as follows:

- Male and female post-stroke volunteers, in the age group of 18-80 years and have normal or corrected to normal vision (e.g. normal vision by using glasses);
- Six months to 3 years post-stroke since the first episode of stroke: this is to capture stroke survivors within the chronic stage and also to ensure that the stage of fast spontaneous recovery has finished;
- Able to follow two-part spoken or written commands: this is to ensure, stroke survivors can provide informed consent and also to ensure, they will be able to comply with therapy;
- Have movement disability in at least one of their hands due to stroke;
- Able to get in and out of a low seat unassisted;
- Ready to remove all body piercings.

The exclusion criteria of the participants are as follows:

- Known to have a progressive neurological condition, any serious medical or psychological diseases which are likely to seriously affect their ability to continue with experimentation;
- Have metal or active implants in their body (excluding dental fillings or crowns);
- Known to suffer from claustrophobia;
- Pregnant or breastfeeding;
- Gross cognitive impairment or disorientation, evidenced by a score of <21 in the Mini-Mental State Examination (MMSE); the MMSE is an 11-item reliable and valid measure of cognitive function [33], such that they are unable to follow verbal or written instruction.

We would like to clarify that we have not involved healthy subjects as a control group in this study. This study is a single-arm trial which is intended to establish CBPT as a biomarker for motor recovery monitoring by longitudinally correlating the motor outcome variations with the CBPT variations across the sessions. We do not need a control group here as we are not validating the clinical effectiveness of the proposed intervention. Establishing clinical effectiveness of CBPT based h-BCI intervention on stroke patients would be the objective of our future work.

C. SYSTEM OVERVIEW & DATA ACQUISITION

The h-BCI system is built on the MATLAB/Simulink platform. It has an interactive graphical user interface (GUI) based front-end for collecting patients' information and storing it in the MS-Access based datastore. The system has a user management module, a training module, a data analysis module, and an online feedback generation module. The training module communicates with a Simulink model running at the backend for collecting the EEG and EMG data and running the experimental training paradigm. The data analysis module is responsible for feature extraction and classifier generation by running a MATLAB script at the backend. This classifier is then used by the online feedback generation module which calls a Simulink model in the background. The algorithm for single-trial based analysis of the acquired data for providing contingent neurofeedback was implemented inside the Simulink s-functions (user-defined function blocks). These functions were also responsible for playing a stop-motion video for virtual hand-grasp (visual neurofeedback) and serial communication with the hand-exoskeleton circuit for sending the control commands linked to the visual feedback. The hand

exoskeleton used in this study is a home-made three-finger exoskeleton capable of providing the flexion and extension motion of the thumb, index, and middle fingers. The index and middle fingers are driven in a coupled fashion by the one link of the exoskeleton while the thumb is driven by another. The links are based on a four-bar mechanism so that the natural human finger trajectory (as they are elliptical rather circular due to an instantaneous change in the centre of rotation) can be maintained. The mechanisms are operated by 2 Hitec HS5685MH servo motors capable of producing 12.9 kg-cm torque at 7.4 V. The hand-exoskeleton is fully wearable, portable, and light-weight (410 g with the battery pack) maintaining usable design specifications prescribed by Pacchierotti *et al.* [34]. It is to be noted that the arm-rests (which helps the exoskeleton resting on a table for rehabilitation use) are easily detachable when portability is needed (such as to be used for activities of daily living).

The EEG and EMG data were acquired using the standard g.USBamp (g.tec, Graz, Austria) biosignal amplifier, along with active ring electrodes (g.LADYbird having sintered Ag/AgCl crown) attached to the EEG cap (g.GAMMAcap). The signal was sampled at 512 Hz and initially band pass filtered over 0.1 Hz to 100 Hz with a notch filter at 50 Hz to avoid the power-line noise. We intended to cover the frontal, medial and parietal regions of the brain apart from the motor cortex as the current sources related to the finger motions are also located in those areas as revealed by joint f-MRI and EEG studies previously [35], [36]. For example, Mizuguchi *et al.* [37] showed the involvement of dorsolateral prefrontal cortex (DLPFC) for motor action planning. Moreover, in stroke patients, the degree of activity decreases in sensorimotor cortex as compared to the pre-stroke motor imagery. It was also found that sensorimotor areas are well connected to the surrounding brain areas such as connectivity of supplementary motor area with DLPFC [38] or the coupling of Premotor area with DLPFC [39]. Therefore, it was essential to explore not only the sensorimotor area but also its surrounding areas. However, we had only a 16 channel device for the data acquisition from which 4 channels had to be allocated for EMG acquisition. Therefore, we are left with 12 EEG channels to cover the motor cortex and the other relevant areas around it as mentioned. Thus we had to compromise on putting the electrodes more centrally of the motor cortex. The 12 EEG electrodes placed around these locations and the placement of the EMG sensors for the data acquisition are shown in Fig. 3. The reference electrode was attached to the left ear-lobe. The placement of the EMG electrodes was on right and left finger flexion muscle group (FFM) (i.e. FFM_R and FFM_L, respectively) in a bipolar fashion, while the reference was taken from the bony part of the elbow. The participants sat on a chair in an upright position at about 0.5m distance from the monitor wearing the exoskeleton in their impaired hand. The intervention exercises were performed for up to 12 sessions spanning over a 5 week period with 2-3 sessions per week.

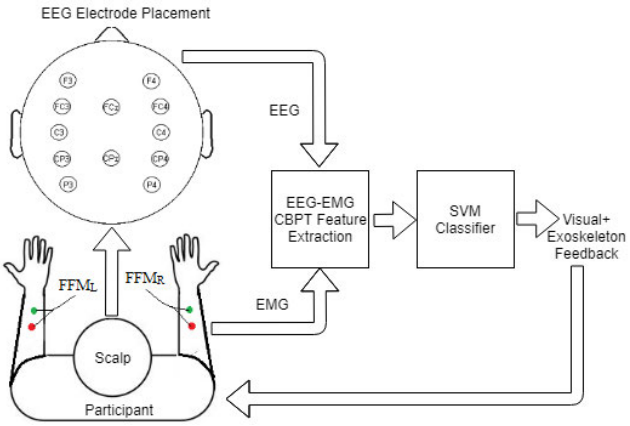

FIGURE 3. The schematic of data acquisition and processing. The EEG channels are shown by magnifying the scalp area of the participant. The EMG channels are shown on the left and right forearms. The arrows are indicating how the EEG and EMG signals are used for CBPT feature extraction and then classification using an SVM classifier. Finally, the classifier predicts the left or right motor attempt to issue multimodal (Visual+Exoskeleton) neurofeedback.

D. INTERVENTION

The intervention consists up to 12 sessions of h-BCI controlled hand-exoskeleton therapy for each participant. The setup for the intervention has been depicted in Fig. 4. Each therapeutic session consists of 2 runs for calibrating the h-BCI system and 3 runs for providing online neurofeedback contingent to the participants' corticomuscular coactivation related to the presented cue during a trial. There were 40 trials in each run of the h-BCI. The timing diagram of a single trial during the calibration and online feedback generation

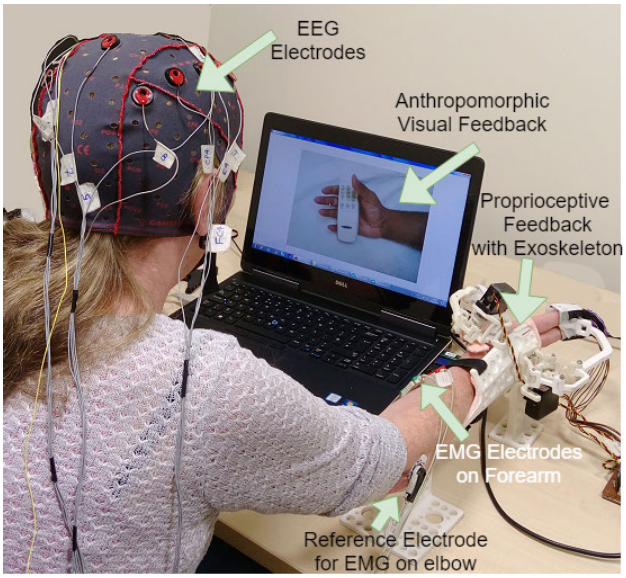

FIGURE 4. The experimental environment is shown here. The participant is wearing the hand exoskeleton on her right (impaired) hand, while the armrest attached with the exoskeleton supporting the forearm to be in a stable position. The participant is getting visual neurofeedback on the computer screen along with exoskeleton based proprioceptive feedback.

stage is shown in Fig. 5. Each trial lasts for 8 s with a random 2 s to 3 s interval as the inter-trial interval (ITI) between the two consecutive trials which makes one run to be roughly 7.5 min. We have chosen an ITI according to our previous studies [12], [28] where it was found to be working well in avoiding the effects of the participants anticipating the timing of the cue. Combining all the runs in a session including the preparation time of the participant (putting the electrodes and other connections) and relaxation between two consecutive runs, it was roughly 1 hr of h-BCI controlled hand-exoskeleton based therapy. Prior to the 1 hr long h-BCI based therapy, participants went through a 30 min of finger opening and closing practice assisted by the exoskeleton to prepare them for the next stage. During the h-BCI based therapy, the participants were asked to make a grasping attempt (either left or right hand depending on the cue) when the cue is presented within a trial. The EEG and the EMG signals related to the grasp-attempt are picked up by electrodes placed on the patient's scalp and forearm muscle and the corticomuscular coactivation is computed using the CBPT method. A classifier is trained during the calibration stage of the session based on the CBPT feature to classify between the left and the right grasp-attempts and the trained classifier is used during the 3 online feedback runs following the calibration. The patients were provided with the visual feedback. If it is the impaired hand, additional feedback is also provided in terms of proprioceptive feedback aligned with the visual feedback using the hand exoskeleton. Proprioception is defined as the sense which enables us to perceive the movement, location, and action of different body parts (here the thumb, index, and middle fingers) according to the Encyclopedia of Neuroscience [40]. We have taken qualitative feedback from the participants to ensure that they were actually able to sense the movement, location, and action of their finger flexion while the exoskeleton was assisting them to perform these motions. Such proprioceptive feedbacks are typically provided by orthoses or exoskeletons for BCI based poststroke therapies [27], [41], without any use of electrical stimulation. As we are dealing with EEG-EMG correlation here we could not use electrical stimulation as that would generate non-volitional EMG activity. As the hand exoskeleton mainly facilitates passive motion [41] of the fingers and does not stimulate the muscle therefore it did not affect the volitional EMG signals.

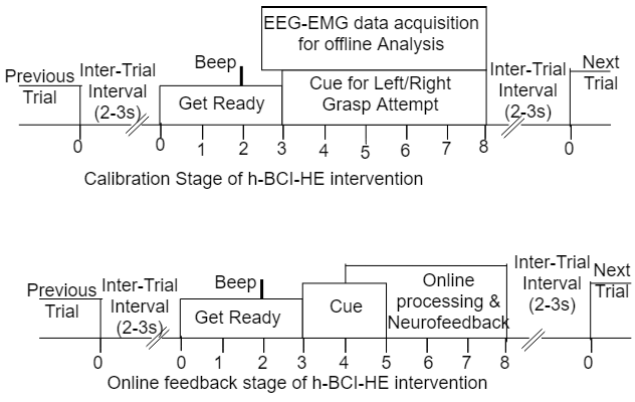

FIGURE 5. Timing Diagram of the experimental protocol. The timing diagram for the calibration stage is shown at the top while the same for the online feedback stage is shown at the bottom. In the online feedback stage, the 3 to 8 s duration is divided into cue display for the first 2 s the rest of the time is used to give neurofeedback by simultaneously processing EEG and EMG data in the background.

E. MOTOR OUTCOME MEASURES

The rehabilitation outcomes were measured every week using the standard motor recovery measures such as ARAT and GS (in kg). There were a total of 5 measurements taken for each participant during the course of the therapy. The ARAT measures 4 basic hand functionality such as grasp (score: 0–18), grip (score: 0–12), pinch (score: 0–18), and gross movements (score: 0–9). Thus the total range of ARAT is 0–57. The total score of each functionality is divided into several tasks which are assigned a score between 0–3. As described by Lyle [42] the measurement of ARAT involves the apparatus such as wooden blocks of different sizes, sharpening stone, cricket ball, glass and jar of water, hollow tubes of different height and thickness, washers, ball bearings, and marbles of different dimensions. A dynamometer is used to take three consecutive measurements and then averaged to get the estimate of the patient's grip-force.

F. DATA ANALYSIS

The acquired EEG and EMG data from the calibration stage of each session are used first to extract the CBPT features which act as a measure of corticomuscular coactivation. These features are then fed into a support-vector-machine (SVM) based classifier to discriminate between the left and right-hand grasp attempts. We have used the in-built function in MATLAB for optimizing the hyper parameters of SVM which uses the Bayesian optimization technique to tune the hyper parameters. A 10-fold cross validation was used during the training process to generate the SVM model. For training, we have used two-third of the dataset and the testing was done on the remaining of one-third of the dataset. The choice of SVM was inspired by the fact that it has been used more frequently in EEG-based BCI studies [43], [44] and also have been found to outperform linear discriminant analysis (LDA), naïve Bayes (NB), and random forest (RF) classifiers [43]–[45]. Our previous work on a similar dataset also showed that SVM has quite stable and satisfactory performance [12], [28]. The feature extraction function is developed in-house while we have used the MATLAB's *svmtrain* and *svmclassify* functions for classifier generation and prediction purposes. A linear kernel was used to generate the SVM model to avoid overfitting. As we mentioned that CBPT acts as a corticomuscular coactivation index, we further investigated whether this index changes in relation to the motor recovery outcome measures, serving as a potential biomarker for recovery. The variation of Mu and Beta event-related

desynchronization/synchronization (ERD/ERS) over the sessions is also calculated and its relation to the motor recovery outcome measures is analyzed for comparing its performance as a biomarker with that of CBPT. It is to be noted that the paired t-test was used for all statistical comparisons keeping the threshold for p-value as 0.05.

1) CBPT FEATURE EXTRACTION AND CLASSIFICATION

A detailed description, rationale and performance of CBPT method as a corticomuscular coactivation index capable of single-trial based prediction of motor-attempt has already been introduced in our previously published work [12]. Here we briefly describe the CBPT method to highlight how the EEG and EMG signals are correlated to build an h-BCI feature. At the first stage the raw EEG ($rEEG_i$) and EMG ($rEMG_i$) data from trial i are bandpass filtered to their respective frequency bands (8-12 Hz for EEG and 30-50 Hz for EMG). Then the bandpass filtered EEG ($bEEG_i$) and EMG ($bEMG_i$) are squared to get the EEG and EMG band-powers ($pEEG_i$ and EMG $pEMG_i$). The bandpower EEG and EMG are then moving-window-averaged with a smoothing kernel of 1 s for EEG ($smEEG_i$) and 32 ms ($smEMG_i$) for EMG. The length of the smoothing window is obtained empirically for optimal performance of the classifier. Then at the last step suitable time-window over the period 3.5 s to 5 s (i.e. +0.5 s to 2 s after the cue) is chosen from $smEEG_i$ and $smEMG_i$ to calculate the Pearson's correlation between these two time-courses. The data from the neurofeedback window was not used for the CBPT calculation as we have found in our previous study [12] that the EEG and EMG signals generally plateau after this point and hence not reliable for drawing a correlation. However, The participants are supposed to maintain a constant grasp throughout the trial period to encourage more engagement with the task. The absolute value of this correlation above the chance level is considered as the CBPT index for that trial ($CBPT_i$). We have used the *corrcoef* function of MATLAB for calculating the correlation coefficient and its $p-$value. If the $p-$value is greater than 0.05, $CBPT_i$ value is not considered and replaced by zero. A feature vector comprising of $CBPT_i$ from all the different EEG and EMG channel combinations is formed for every trial within the calibration stage and then fed into the SVM model for classifier training. At the online feedback stage, the same CBPT feature extraction process is repeated and classified by the trained SVM classifier. The CBPT feature vector was 10 dimensional which comprised of the following EEG-EMG channel combinations: $F3-FFM_R$, $FC3-FFM_R$, $C3-FFM_R$, $CP3-FFM_R$, $P3-FFM_R$, $F4-FFM_L$, $FC4$-FFM_L, $C4-FFM_L$, $CP4-FFM_L$, $P4-FFM_L$. It is to be noted that the beta CBPT was not used during the online BCI task. It was the mu CBPT which was used during the actual experimentation in online BCI mode. The beta CBPT was calculated during the offline analysis of the raw signal in the similar manner as mu in online, as both these bands (mu and beta) are related to motor actions and we wanted to present a broader picture of CBPT's association with motor recovery.

2) BIOMARKERS RELATED TO THE RECOVERY

The neurophysiological markers of recovery are calculated in two ways. First, whether the CBPT indexes can reflect the dynamical changes in recovery and then we compared it with the existing measure of changes in recovery as the variation of Mu and Beta band-power. The average CBPT index between the EEG channels and impaired hand EMG is calculated for each session and then it is correlated with the motor recovery measures GS and ARAT. The same is also repeated with the Mu and Beta band-power measures where the average Mu and Beta ERD/ERS are calculated for every session related to the motor attempt of the impaired hand. The ERD/ERS is calculated according to the following formula.

$$ERD/ERS_b^{ch} = \frac{E^b task}{E^b ref} \tag{1}$$

The ratio between the average band-power during the motor-attempt and the reference period is defined by (1), where ch denotes the EEG channel and b denotes the band (Mu or Beta). The numerator in the right-hand side of (1) is the average bandpower during the motor attempt period (averaged over 0.5 s to 1.5 s after the cue) and the denominator is the average bandpower during the reference or resting period (averaged over 1.5 s to 0.5 s before the cue). The choice of the time spans of $E^b ref$ and $E^b task$ were inspired by the previous literature including our own work [28], [46]. Basically we needed to find two time spans one before the cue and another after the cue where the bandpower variations were stable and plateaued. In our previous clinical trial with similar experimental paradigm we have used a $E^b ref$ time frame 0.5 s before cue [28] which gave stable measurement of ERD/ERS for patients with similar type of disability. It was also observed in the previous literature that the maximal magnitude of ERD occurs 0.4 s after the cue [46] which could be a good choice for calculating $E^b task$. Thus a time span 0.5 s before the cue and 0.5 s after the cue was decided for $E^b ref$ and $E^b task$ respectively. We also wanted to keep parity on the number of samples used for the averaging of the bandpower. Hence, we experimentally decided upon a 1 s time period for the bandpower averaging. Thus the bandpower was averaged between 1.5 s and 0.5 s before the cue for $E^b ref$ and for $E^b task$ it was averaged between 0.5 s and 1.5 s after the cue. It is noteworthy that the motor recovery assessments (GS and ARAT) are taken weekly (5 in total) and the biomarkers based on CBPT and ERD/ERS were calculated per session. Therefore, to match the number of time points in both the time-series (motor-recovery and biomarker) for the sake of correlation calculation, the average over all the sessions (for the biomarkers) which fall within a week are considered as one time-point. The correlations were calculated for each of the EEG channels and correlation coefficient for which $p-$value is greater than 0.05 is not considered and replaced by zero.

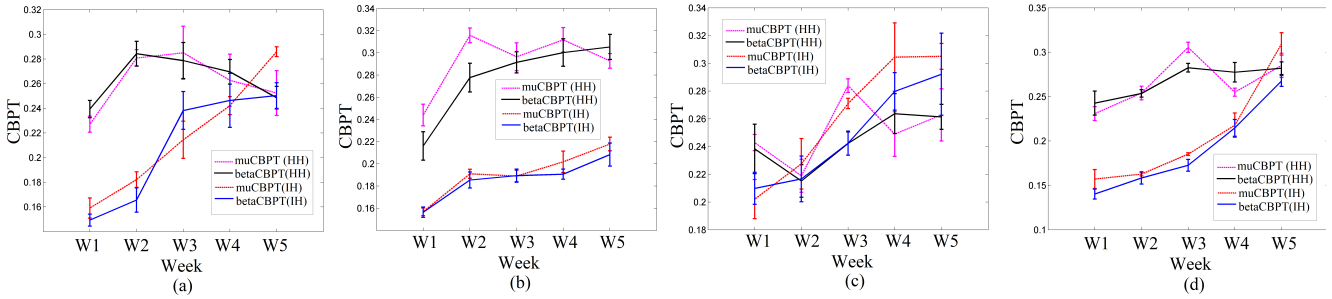

FIGURE 6. CBPT variations of all the participants: (a) S01, (b) S02, (c) S03, (d) S04. Each point in the graphs represents the mean CBPT across the EEG channels and the errorbar represents its standard deviation. The legends having HH and IH in parenthesis show the variations for healthy hand and impaired hand respectively for individual participants. For participant S01 and S04, we can see clearly that the CBPT differences between the healthy and impaired hand decrease gradually with the increase in treatment time.

III. RESULTS

The accuracy of the h-BCI for generating the neurofeedback associated with the motor task has already been reported in a previous conference paper [47]. So, here we briefly mention those results to set the background of the further results presented in this paper. All the participants were able to control the exoskeleton with higher accuracy as the therapeutic session progresses. The group-mean increase in accuracy was +19.01% from the first session (58.16±7.81%) to the last session (77.17±3.65%). The motor outcome measures ARAT and GS showed a group-mean change of +23.75 in ARAT and +9.83 kg in GS. Both of these positive changes are found to be statistically significant ($p-$value<0.05). Interestingly, the improvement in ARAT and GS exceeded the minimal clinically important difference (MCID) limit [48] of 5 and 6.2 kg respectively.

A. RELATIONSHIP OF CBPT WITH RECOVERY OUTCOME

The CBPT variations throughout the therapy have been shown in Fig. 6(a)-(d), for participants S01, S02, S03, S04 accordingly. These plots were generated by taking the average and standard deviation of the contralateral CBPT for the impaired hand. The standard deviations are represented by the errorbars for each such points. It is to be noted from the plots that for all the participants the average CBPT has increased from the first week to the last week. The group-mean changes in CBPT(Mu band) and CBPT(Beta band) are +0.11 and +0.09 respectively; both of them statistically significant ($p-$value<0.05). Moreover, we can see that for participant S01 and S04 the CBPT difference between healthy and impaired hand is gradually decreasing as the treatment progresses. However, for S02 and S03 this pattern is not very clear. This could be due to the fact that we are comparing two different hands, left and right, and there may be an initial difference between the dexterity which may vary across the participants. Also, the amount of overall gain in CBPT due to motor skill learning could play a factor here as we can see that the changes in CBPT are a bit higher for S01 and S04 than in S02 and S03. Therefore, a control group with the same hand as the dominant hand would be necessary for a true comparison. But overall, we can see that the CBPT is gradually improving to become closer to the healthy hand CBPT as the therapy progresses.

The relationship of CBPT changes at different EEG-EMG channel pairs is also correlated with the motor recovery outcomes and the topoplots are generated to see their distributions over the scalp. These topoplots are shown in Fig. 7 (a)-(d) for participants S01, S02, S03 and S04 respectively. The scatter plots of correlations corresponding to each topoplots can be seen in Fig. 8(a)-(d) for participants S01, S02, S03, and S04 respectively. The variation of the CBPT with the GS and ARAT measures are also shown as scatter plots with a trendline (linear least-square) in Fig. 8 where the values of the significant ($p-$value<0.05) correlation-coefficients are mentioned in the labels for each channel. For participant S01 (Fig. 7(a) and Fig. 8(a)) statistically significant ($p-$value<0.05) correlations are found between the CBPT(Mu band) variations and GS variations over the weeks for the EEG channels F3, FC3, and C3 and EMG channel (FFM_R). For CBPT(Beta band) statistically significant ($p-$value<0.05) correlation is found in F3. The CBPT(Mu band) and CBPT(Beta band) are also significantly ($p-$value<0.05) correlated with ARAT scores for all the contralateral EEG channels F3, FC3, C3, CP3, and P3, while for CBPT(Beta band) it is significant ($p-$value<0.05) in F3, CP3, and P3. Here the significant correlations are all beyond 0.90.

The correlations of CBPT(Mu band) with GS for S02 (Fig. 7 (b) and Fig. 8(b)) are found to be significant ($p-$value<0.05) at F4 and P4 while for CBPT(Beta band) it was significant ($p-$value<0.05) at FC4 and CP4. Again, the correlations between CBPT(Mu band) and ARAT are significant ($p-$value<0.05) at F4, C4, and P4, while it is significant ($p-$value<0.05) at F4, CP4, and P4 for CBPT(Beta band) vs. ARAT.

The results from S03 (Fig. 7 (c) and Fig. 8(c)) shows that there are significant ($p-$value<0.05) correlation between CBPT(Mu and Beta band) and GS for F3. The correlations of CBPT(Mu band) with ARAT scores are found to be significant ($p-$value<0.05) at F3, C3, CP3, P3, while in the

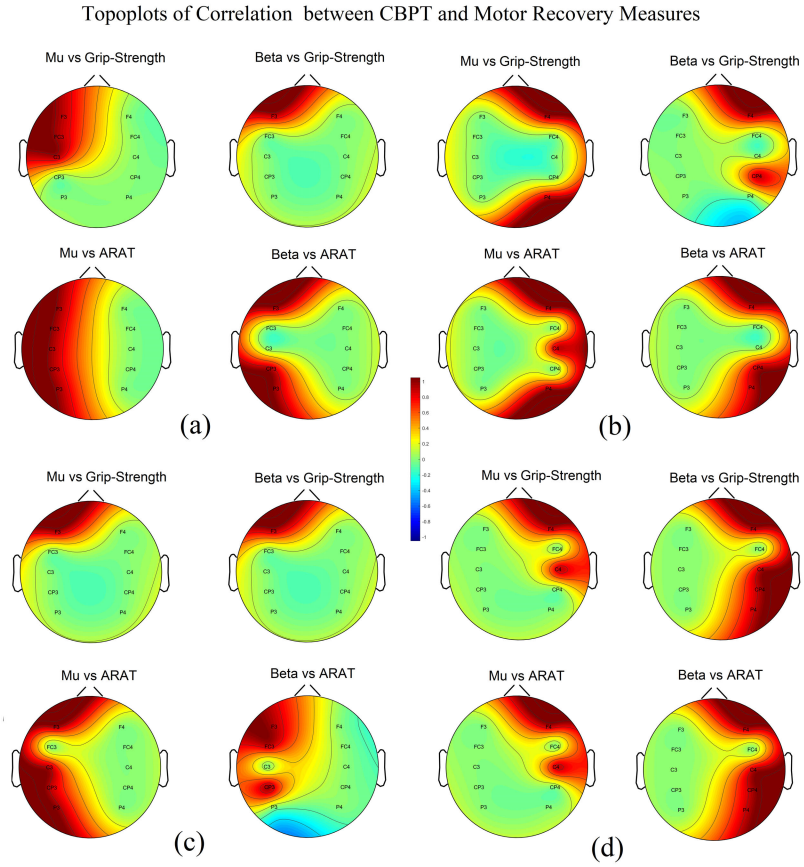

FIGURE 7. Topoplots of correlations between CBPT and motor outcome measures for (a) S01, (b) S02, (c) S03, and (d) S04. It is to be noted that S01 and S03 were impaired by their right side, while S02 and S04 were impaired by their left side.

case of CBPT(Beta band) and ARAT statistically significant ($p-$value<0.05) correlations are found at F3, FC3 and CP3.

The CBPT(Mu band) correlations with GS and ARAT show significant ($p-$value<0.05) relation only at F4 and C4 for S04 (Fig. 7 (d) and Fig. 8(d)), where the coefficients are all above 0.89, although correlations between CBPT(Beta band) with GS and ARAT are found significant ($p-$value<0.05) at F4, C4, CP4, and P4 where the coefficients are also above 0.89.

B. RELATIONSHIP OF BANDPOWER VARIATION WITH RECOVERY OUTCOME

The week-wise bandpower analysis in terms of ERD/ERS has shown (Fig. 9(a)-(d)) an overall trend of decrement for both the bands (Mu and Beta). Each point on these graphs represents the average ERD/ERS across all the channels and the vertical errorbars represent the standard deviation of ERD/ERS across all the channels. The group-mean change of -0.18 in Beta ERD/ERS is also found to be statistically significant ($p-$value<0.05) as it reduced 17.20% from the baseline. In Mu band, ERD/ERS, a significant ($p-$value<0.05) change of -28.36% was also observed as the group-mean changed (-0.29) from 1.03 to 0.74.

An investigation on how the Mu and Beta bandpower (i.e. ERD/ERS) variations are related to the motor outcome measures (GS and ARAT) shows that there are significant ($p-$value<0.05) correlations at various EEG channel locations on the scalp. The scalp topoplots of correlations are shown in Fig. 10(a)-(d) and their corresponding scatter plots can be seen in Fig. 11(a)-(d) respectively for participant S01 to S04. The variation of the ERD/ERS with the GS and ARAT measures are also shown as scatter plots with a trendline (linear least-square) beside every topoplot where the values of the significant ($p-$value<0.05) correlation-coefficients are mentioned in the labels for each channel. We have taken the absolute values of the correlation to keep uniformity in representation for both the CBPT and bandpower measures. The Beta band ERD/ERS are found to be significantly correlated ($p-$value<0.05) with the GS and ARAT scores at the EEG channels ipsilateral to the impaired hand (right hand) for the participant S01 (Fig. 10(a) and Fig. 11(a)). For example in relation to the GS it is significant at ipsilateral: FC4, C4, CP4, central: FCz and CPz. The correlations of Beta band ERD/ERS with ARAT scores for S01 shows that the coefficients are significant ($p-$value<0.05) at ipsilateral: FC4, C4, CP4,

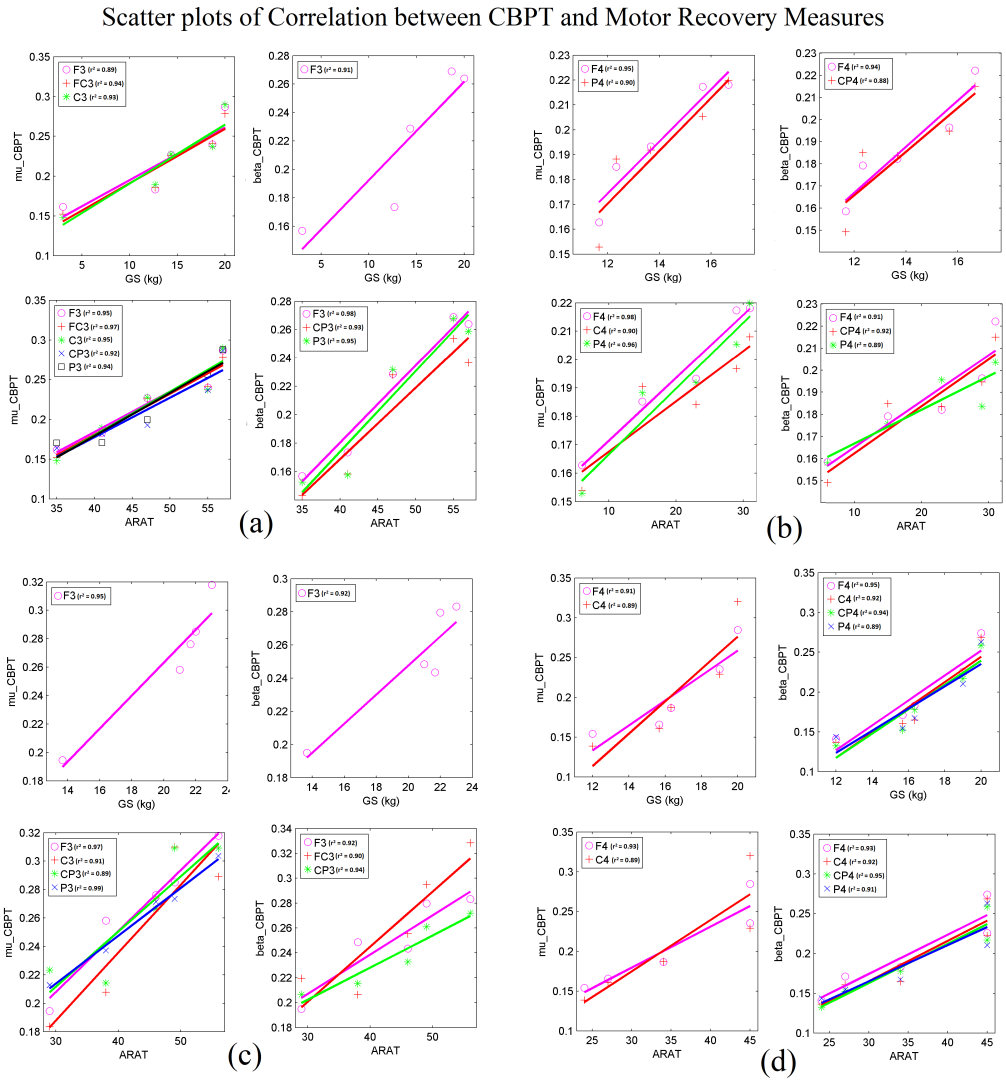

FIGURE 8. Scatter plots of correlations between CBPT and motor outcome measures for (a) S01, (b) S02, (c) S03, and (d) S04. It is to be noted that S01 and S03 were impaired by their right side, while S02 and S04 were impaired by their left side.

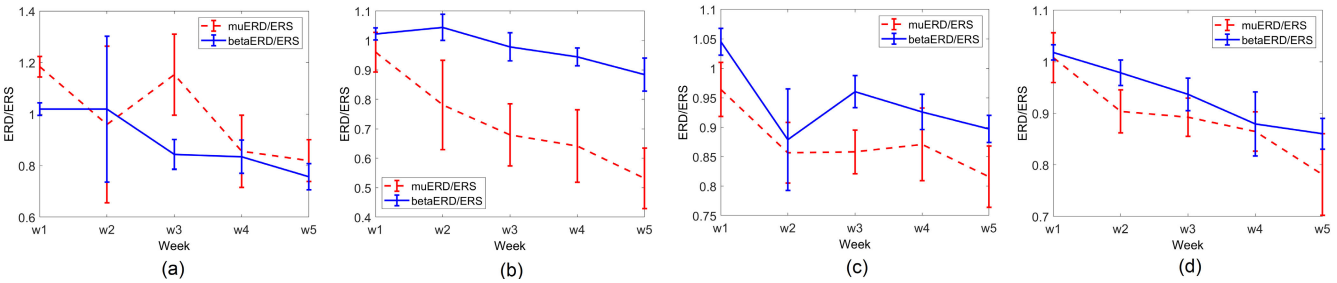

FIGURE 9. ERD/ERS variations of all the participants: (a) S01, (b) S02, (c) S03, (d) S04. Each point on these graphs represent the average ERD/ERS across all the EEG channels and the vertical errorbars represent the standard deviation of ERD/ERS across all the EEG channels.

contralateral: CP3, Central: FCz and CPz. In contrast, the Mu band power variations show contralateral pattern as significant ($p-$value<0.05) correlation is found at CP3 and P3 for GS and CP3 for ARAT.

For the participant, S02 (Fig. 10(b) and Fig. 11(b)), Beta band ERD/ERS is found to be significantly ($p-$value<0.05) correlated with GS scores at the EEG channels; contralateral (S02 is impaired at the left hand): FC4 and CP4, Central: FCz,

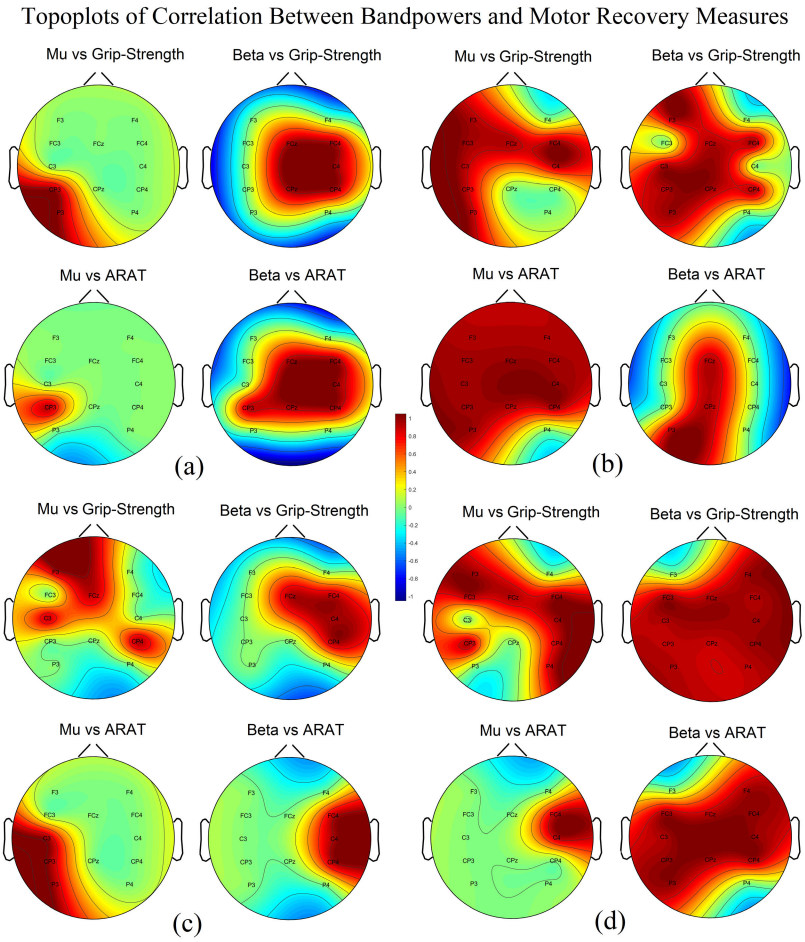

FIGURE 10. Topoplots of correlations between ERD/ERS and motor outcome measures for (a) S01, (b) S02, (c) S03, and (d) S04. It is to be noted that S01 and S03 were impaired by their right side, while S02 and S04 were impaired by their left side. Although the original correlation-coefficients are negative (see scatter plots in Fig. 11), the topoplots are shown as positive with the same values just to compare it with CBPT correlations.

CPz and ipsilateral: F3, C3, CP3, P3. Beta band ERD/ERS correlated with ARAT only at ipsilateral: P3 and central: FCz and CPz EEG channels, while none of the contralateral channels are significant. The Mu band ERD/ERS relation with GS also followed the ipsilateral pattern, as significant ($p-$value<0.05) correlation is found in all the ipsilateral (F3, FC3, C3, CP3, and P3) EEG channels (r>0.89), along with central: FCz and contralateral: FC4 and C4. For Mu band ERD/ERS relation with ARAT, a bilateral pattern is observed with r being insignificant ($p-$value>0.05) only at P4.

The correlations of Beta band power variation with the GS and ARAT measures are found to be significant mostly in ipsilateral (as S03 was impaired by the right hand) EEG channels for S03 (Fig. 10(c) and Fig. 11(c)). For GS significant ($p-$value<0.05) correlations are at FC4, C4, CP4, and FCz, while for ARAT significant ($p-$value<0.05) correlations are at FC4, C4, CP4. In contrast to this, the Mu band correlations are mostly at the contralateral side as significant ($p-$value<0.05) correlations are at FC3, C3, FCz, and CP4 for GS and C3, CP3, and P3 for ARAT.

A bilateral pattern is observed for the relationship of Beta band power with GS and ARAT for S04 (Fig. 10(d) and Fig. 11(d)). Significant ($p-$value<0.05) correlations (r>0.89) are found for all the EEG channels except F3 for GS and F3 and P4 for ARAT. The Mu band correlations with GS are also found to be bilateral as significant ($p-$value<0.05) correlations are observed in F3, FC3, CP3, FCz, FC4, C4, CP4, and P4. However, the correlations between Mu band-power and ARAT are significant only at contralateral EEG channels FC4 and C4.

In Fig. 12 we have averaged the Figs 7(a)-(d) and Figs 10(a)-(d) (after lateralizing it to the left hemisphere as the lesion side for the sake of comparability) to clarify the interpretation of the results across the subjects. Although inter-subject variability which is a common phenomenon in EEG sometimes makes such plots blurry, Fig. 12 shows consistency in terms of neurophysiology as we can see significant

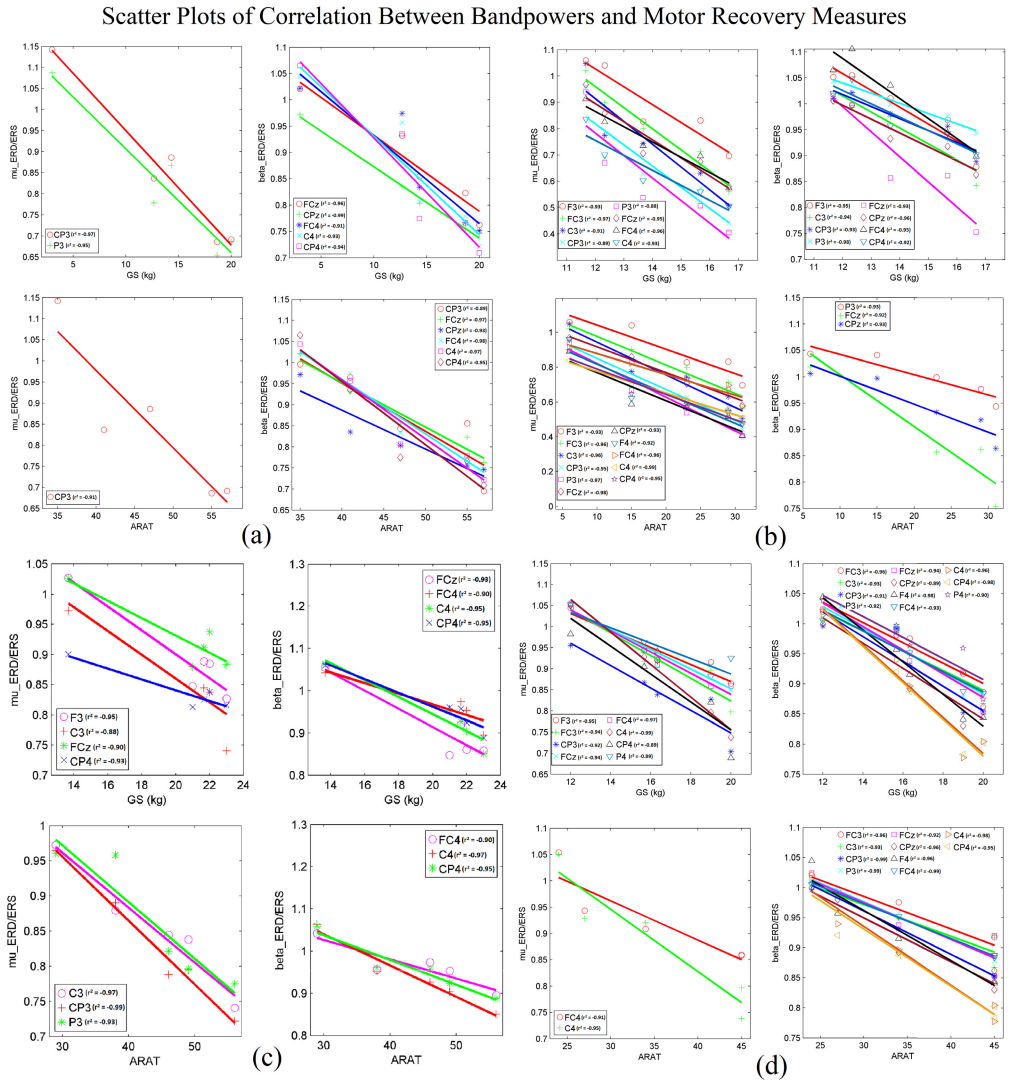

FIGURE 11. Scatter plots of correlations between ERD/ERS and motor outcome measures for (a) S01, (b) S02, (c) S03, and (d) S04. It is to be noted that S01 and S03 were impaired by their right side, while S02 and S04 were impaired by their left side.

correlations are clustered contralaterally (contralateral to the impaired hand) in Mu-ERD/ERS, and also in Mu-CBPT and Beta-CBPT, when corrected for lateralization.

IV. DISCUSSION

We would like to clarify that this paper does not intend to establish the clinical effectiveness of the CBPT based h-BCI system on the basis of these positive motor outcomes as several factors other than the intervention may have contributed to this and a controlled study with a larger cohort is needed even to make a speculative comment. Therefore only the relevance of CBPT in the context of motor recovery monitoring is discussed in this paper, which is important to warrant further investigation into the clinical effectivity aspect.

A major indication that the variation of CBPT indexes can be used as a biomarker for recovery comes from the observation of the scatter plots (Fig. 8(a)-(d)) that in the case of all the participants, the CBPT indexes increased as the motor outcomes (GS and ARAT) improved. Thus CBPT indexes as a measure of corticomuscular coactivation reveal a stronger correlation between the brain (EEG) and muscle (EMG) signals as the stroke patients regain their motor ability. A similar change in corticomuscular coupling with the motor recovery was also observed in the case of corticomuscular coherence (CMC) measurements in the past [30], [49], [50]. However, CMC based h-BCI was not able to provide sufficient BCI control accuracy as revealed by our previous work [12], whereas CBPT significantly ($p<0.05$) outperformed CMC in controlling a hand-exoskeleton device by the stroke patients. In the current study also, CBPT shows a satisfactory performance as the average accuracy improved significantly ($p-$value<0.05) from the first to the last week

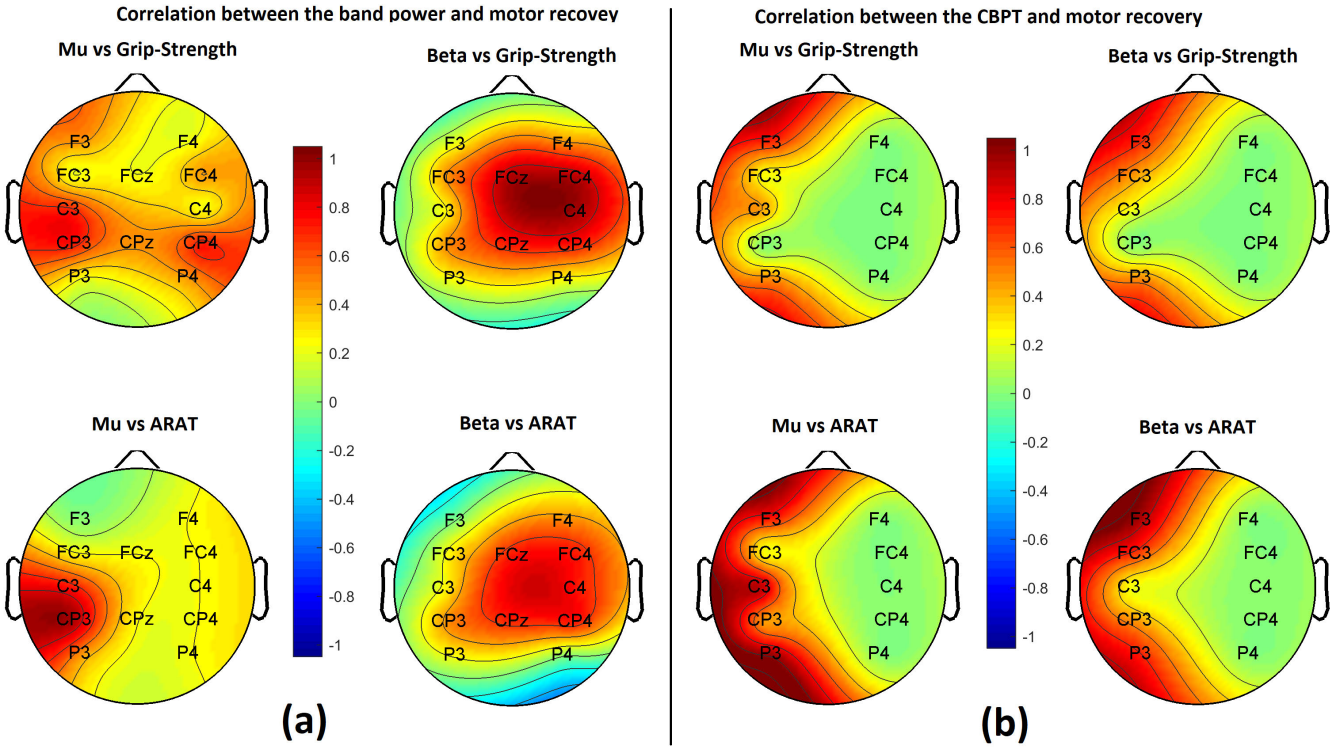

FIGURE 12. Scalp topoplots of correlations averaged across all the participants (a) ERD/ERS and motor recovery, (b) CBPT and motor recovery.

of the therapy. It is important to note that this performance was achieved without any BCI screening. Thus it further reinforces the fact that CBPT based h-BCI architecture is able to improve classification beyond the recommended threshold accuracy level of 70% [51]. This is very important in a rehabilitation setting as the patients may have alterations in their brain activity at the initial stages which limits their BCI performance.

The beta band corticomuscular coupling is only reported in the literature so far, whereas in this paper we have reported the corticomuscular interactions both in Mu and Beta bands. The reason lies in the fact that CMC only looks for coupling between the same frequency of EEG and EMG while it can be present in two different frequency bands. For example, it is well known that motor-actions (motor imagery or execution) related modulations occur in terms of ERD in Mu band (8-12 Hz) [52], which may also influence the EMG activations. However, CMC at this frequency range (8-12 Hz) is not visible because EMG activations are prominent at a higher frequency range as its power spectrum peaks around 50–60 Hz [53]. Therefore motor action related EEG modulations occur at a bit higher frequency range (beta rhythms: 15-30 Hz) which overlaps with the spectrum of EMG activations and this contributes towards a significant level of CMC. This limitation is overcome by the CBPT, which can look at the cross-frequency interactions between EEG and EMG, and hence an investigation of corticomuscular correlation at both the Mu and Beta bands is possible.

The comparison with the variations in sensory motor rhythm (SMR) has also been made in terms of Mu and Beta band ERD/ERS changes over the therapeutic period. As there is a general consensus that the changes in beta bandpower is a significant biomarker for motor recovery [41], [54], this comparison further validates that the variations in CBPT are meaningful. Here we also found that not only the beta band ERD/ERS but also the Mu band ERD/ERS is correlated with the motor outcome measures. The contralateral pattern of the SMR (especially in Mu band when averaged across the participants, Fig. 12 (a)) correlations are also evident in the CBPT correlations (in both Mu and Beta band, Fig. 12 (b)). This outcome is also in accordance with the study conducted by Chen and Schlaug where they found increased resting-state fMRI connectivity in ipsilesional motor cortex after the intervention [55]. Although the contralateral pattern is found for all the participants except S02 in the case of Mu ERD/ERS, for Beta ERD/ERS it is ipsilateral for all the participants except S04. Bilateral correlations are also observed particularly in the case of Mu band in S02 and Beta band in S04. Previous findings also showed that corticomuscular coupling is particularly explored to detect neuronal plasticity [30], although the CMC changes didn't correlate with the motor recovery. Such finding is also supported by another study on early phase recovery of poststroke hand functionality where CMC did not perform as an efficient biomarker for recovery [56]. Moreover, a large inter-subject variability was also present there. In our case, CBPT based

corticomuscular coactivation measure shows a much-reduced variability as the contralateral pattern was intact in all participants. More importantly, a strong correlation is also present between the CBPT variations and motor outcomes across the therapeutic period. Indeed, this analysis also sheds light on the continuous changes of corticomuscular correlation during the progress of rehabilitation, whereas other clinical studies mostly reported only the pre- and post-therapeutic changes.

The fact that both the bandpower related changes (Mu and Beta ERD/ERS) and CBPT are found to be strongly correlated with motor outcome measures, indicates a neurophysiological link between them as a biomarker of motor recovery. The bi-lesional pattern of the bandpower related correlations, occurring in a few instances, maybe due to the involvement of a wide range of cortical regions influencing muscle activity, which was found in a previous study [57]. The increment in CBPT cannot be credited to the gross enhancement in the EMG amplitude or gross decrement in the Mu bandpower (ERD/ERS). This is evident from the very definition of CBPT method (presented in section II-F1) that the CBPT index depends on the correlation between the band-limited power time-courses of EEG and EMG and not the overall amplitude changes. Hence, enhanced CBPT is attributed to the gradual improvement in the stability of simultaneous EEG and EMG activations relating to the motor attempts, over the course of therapy. We also argue here that the mode of designing a restorative BCI should consider the factors affecting the rehabilitation process, as we have designed our h-BCI using CBPT which showed a strong correlation with motor outcome measures.

It can be argued that a simple EMG feature extraction would have worked for classifying left vs. right-hand task in this case as the patients had residual EMG activity. However, it is to be noted that the purpose of this study is not just to provide a means for issuing high fidelity neurofeedback to the patients. The study is inspired by the fact that the connectivity between the central and peripheral nervous system (or corticomuscular coupling) plays an important role in the motor recovery process as revealed by the studies on corticomuscular coherence (CMC) analysis [18]. But unfortunately, CMC is not suitable for single-trial based prediction due to high inter-trial variability. Hence, our previous study [12] tested whether a new measurement namely CBPT can solve this issue of single-trial detectability. Nevertheless, the ultimate aim of developing such a method would be unfulfilled if it hasn't been tested for its impact on the motor recovery process, more like CMC. Therefore, it was necessary to drive the neurofeedback using CBPT rather than by EMG activity only, so that the corticomuscular connectivity can be captured and its change throughout the therapeutic process can be correlated with the motor-outcome measures in order to investigate its impact on recovery. Although the work presented in the paper deals with signals related to motor-attempt, another major aspect worth exploring in future investigations is the effect of pre-movement on corticomuscular coactivation. Pre-movement features such as movement-related cortical potentials (MRCP) is quite useful for high performing BCI design [58], which can be used to predict corticomuscular coactivation for h-BCI based rehabilitation.

Given the fact that the study was conducted on chronic stroke patients whose recovery had stopped for a long time it is interesting to see the recovery process restarted as the intervention was applied. Again, such observations do not lead to any conclusion regarding the clinical effectiveness of the intervention rather it only warrants a further investigation using controlled trials on a larger cohort. Nevertheless, the study does advocate for the fact that CBPT can serve as a biomarker for motor recovery monitoring as it showed a strong correlation with the motor outcome measures and the topographic patterns of the correlation also conform to the neurophysiological signatures found in previous studies.

V. CONCLUSION

The pilot trial presented in this paper showed that the CBPT, as a measurement of corticomuscular co-activation behaves similarly to a neurophysiological marker for motor recovery monitoring as revealed by its strong correlation with the dynamic changes in motor outcome measures during the therapeutic process. This is also a pioneering study where a corticomuscular co-activation feature (CBPT) is used for an h-BCI driven rehabilitation therapy for the first time while the same feature is used as a potential biomarker for motor recovery. The significant positive changes in the motor outcome measures are also noteworthy since the patients were in the chronic stage with the recovery process stopped for long before the intervention. However the clinical effectiveness of the given intervention is inconclusive unless a controlled trial with a larger patient cohort is performed in future.

ACKNOWLEDGMENT

The authors would like to thank Ms. Annmarie Kelly, Occupational Therapist, Altnagelvin Hospital, Derry-Londonderry, for helping in patient recruitment, Prof. Suzzane McDonough for suggesting the motor outcome measures, and Dr. Yogesh Kumar Meena for helping in the data collection process. They also thank Mr. Shyam Sunder Nishad for designing the hand exoskeleton.

REFERENCES

[1] G. Pfurtscheller, "The hybrid BCI," *Frontiers Neurosci.*, vol. 4, p. 3, Apr. 2010.

[2] B. Z. Allison, "Toward a hybrid brain–computer interface based on imagined movement and visual attention," *J. Neural Eng.*, vol. 7, no. 2, Mar. 2010, Art. no. 026007.

[3] T. Yu, J. Xiao, F. Wang, R. Zhang, Z. Gu, A. Cichocki, and Y. Li, "Enhanced motor imagery training using a hybrid BCI with feedback," *IEEE Trans. Biomed. Eng.*, vol. 62, no. 7, pp. 1706–1717, Jul. 2015.

[4] G. Pfurtscheller, "Self-paced operation of an SSVEP-based orthosis with and without an imagery-based 'Brain switch:' A feasibility study towards a hybrid BCI," *IEEE Trans. Neural Syst. Rehabil. Eng.*, vol. 18, no. 4, pp. 409–414, Aug. 2010.

[5] G. Pfurtscheller, "Functional brain imaging based on ERD/ERS," *Vis. Res.*, vol. 41, nos. 10–11, pp. 1257–1260, May 2001.

[6] R. Vilimek and T. O. Zander, "BC(eye): Combining eye-gaze input with brain-computer interaction," in *Universal Access in Human-Computer Interaction. Intelligent and Ubiquitous Interaction Environments*. Berlin, Germany: Springer, 2009, pp. 593–602.
[7] R. Scherer, G. R. Müller-Putz, and G. Pfurtscheller, "Self-initiation of EEG-based brain–computer communication using the heart rate response," *J. Neural Eng.*, vol. 4, no. 4, pp. L23–L29, Nov. 2007.
[8] C. Cui, G.-B. Bian, Z.-G. Hou, J. Zhao, and H. Zhou, "A multimodal framework based on integration of cortical and muscular activities for decoding human intentions about lower limb motions," *IEEE Trans. Biomed. Circuits Syst.*, vol. 11, no. 4, pp. 889–899, Aug. 2017.
[9] L. Yao, J. Meng, D. Zhang, X. Sheng, and X. Zhu, "Combining motor imagery with selective sensation toward a hybrid-modality BCI," *IEEE Trans. Biomed. Eng.*, vol. 61, no. 8, pp. 2304–2312, Aug. 2014.
[10] L. Minati, N. Yoshimura, and Y. Koike, "Hybrid control of a vision-guided robot arm by EOG, EMG, EEG biosignals and head movement acquired via a consumer-grade wearable device," *IEEE Access*, vol. 4, pp. 9528–9541, 2016.
[11] K.-S. Hong and M. J. Khan, "Hybrid brain–computer interface techniques for improved classification accuracy and increased number of commands: A review," *Frontiers Neurorobot.*, vol. 11, p. 35, Jul. 2017.
[12] A. Chowdhury, H. Raza, Y. K. Meena, A. Dutta, and G. Prasad, "An EEG-EMG correlation-based brain-computer interface for hand orthosis supported neuro-rehabilitation," *J. Neurosci. Methods*, vol. 312, pp. 1–11, Jan. 2019.
[13] R. Leeb, H. Sagha, R. Chavarriaga, and J. R. del Millán, "A hybrid brain–computer interface based on the fusion of electroencephalographic and electromyographic activities," *J. Neural Eng.*, vol. 8, no. 2, Mar. 2011, Art. no. 025011.
[14] R. Kristeva, L. Patino, and W. Omlor, "Beta-range cortical motor spectral power and corticomuscular coherence as a mechanism for effective corticospinal interaction during steady-state motor output," *NeuroImage*, vol. 36, no. 3, pp. 785–792, Jul. 2007.
[15] X. Lou, S. Xiao, Y. Qi, X. Hu, and Y. Wang, "Corticomuscular coherence analysis on hand movement distinction for active rehabilitation," *Comput. Math. Methods Med.*, vol. 2013, Apr. 2013, Art. no. 908591.
[16] Y. Zheng, Y. Peng, G. Xu, L. Li, and J. Wang, "Using corticomuscular coherence to reflect function recovery of paretic upper limb after stroke: A case study," *Frontiers Neurol.*, vol. 8, p. 728, Jan. 2018. [Online]. Available: https://www.frontiersin.org/article/10.3389/fneur.2017.00728
[17] K. von Carlowitz-Ghori, Z. Bayraktaroglu, F. U. Hohlefeld, F. Losch, G. Curio, and V. V. Nikulin, "Corticomuscular coherence in acute and chronic stroke," *Clin. Neurophysiol.*, vol. 125, no. 6, pp. 1182–1191, Jun. 2014.
[18] R. Krauth, J. Schwertner, S. Vogt, S. Lindquist, M. Sailer, A. Sickert, J. Lamprecht, S. Perdikis, T. Corbet, J. D. R. Millán, H. Hinrichs, H.-J. Heinze, and C. M. Sweeney-Reed, "Cortico-muscular coherence is reduced acutely post-stroke and increases bilaterally during motor recovery: A pilot study," *Frontiers Neurol.*, vol. 10, p. 126, Feb. 2019.
[19] Y. Hashimoto, J. Ushiba, A. Kimura, M. Liu, and Y. Tomita, "Correlation between EEG-EMG coherence during isometric contraction and its imaginary execution," *Acta Neurobiol. Exp. (Wars)*, vol. 70, no. 1, pp. 76–85, 2010.
[20] K. von Carlowitz-Ghori, Z. Bayraktaroglu, G. Waterstraat, G. Curio, and V. V. Nikulin, "Voluntary control of corticomuscular coherence through neurofeedback: A proof-of-principle study in healthy subjects," *Neuroscience*, vol. 290, pp. 243–254, Apr. 2015.
[21] X. Lou, S. Xiao, Y. Qi, X. Hu, and Y. Wang, "Corticomuscular coherence analysis on hand movement distinction for active rehabilitation," *Comput. Math. Methods Med.*, vol. 2013, Apr. 2013, Art. no. 908591.
[22] S. F. Farmer, F. D. Bremner, D. M. Halliday, J. R. Rosenberg, and J. A. Stephens, "The frequency content of common synaptic inputs to motoneurones studied during voluntary isometric contraction in man," *J. Physiol.*, vol. 470, no. 1, pp. 127–155, 1993.
[23] D. Tuncel, A. Dizibuyuk, and M. K. Kiymik, "Time frequency based coherence analysis between EEG and EMG activities in fatigue duration," *J. Med. Syst.*, vol. 34, no. 2, pp. 131–138, Apr. 2010.
[24] A. Chwodhury, H. Raza, A. Dutta, S. S. Nishad, A. Saxena, and G. Prasad, "A study on cortico-muscular coupling in finger motions for exoskeleton assisted neuro-rehabilitation," in *Proc. 37th Annu. Int. Conf. IEEE Eng. Med. Biol. Soc. (EMBC)*, Aug. 2015, pp. 4610–4614.
[25] R. Rupp, M. Rohm, M. Schneiders, A. Kreilinger, and G. R. Muller-Putz, "Functional rehabilitation of the paralyzed upper extremity after spinal cord injury by noninvasive hybrid neuroprostheses," *Proc. IEEE*, vol. 103, no. 6, pp. 954–968, Jun. 2015.
[26] G. Morone, I. Pisotta, F. Pichiorri, S. Kleih, S. Paolucci, M. Molinari, F. Cincotti, A. Kübler, and D. Mattia, "Proof of principle of a brain-computer interface approach to support poststroke arm rehabilitation in hospitalized patients: Design, acceptability, and usability," *Arch. Phys. Med. Rehabil.*, vol. 96, no. 3, pp. S71–S78, Mar. 2015.
[27] D. T. Bundy, "Contralesional brain–computer interface control of a powered exoskeleton for motor recovery in chronic stroke survivors," *Stroke*, vol. 48, no. 7, pp. 1908–1915, 2017.
[28] A. Chowdhury, Y. K. Meena, H. Raza, B. Bhushan, A. K. Uttam, N. Pandey, A. A. Hashmi, A. Bajpai, A. Dutta, and G. Prasad, "Active physical practice followed by mental practice using BCI-driven hand exoskeleton: A pilot trial for clinical effectiveness and usability," *IEEE J. Biomed. Health Informat.*, vol. 22, no. 6, pp. 1786–1795, Nov. 2018.
[29] T. Kawase, T. Sakurada, Y. Koike, and K. Kansaku, "A hybrid BMI-based exoskeleton for paresis: EMG control for assisting arm movements," *J. Neural Eng.*, vol. 14, no. 1, Jan. 2017, Art. no. 016015.
[30] P. Belardinelli, L. Laer, E. Ortiz, C. Braun, and A. Gharabaghi, "Plasticity of premotor cortico-muscular coherence in severely impaired stroke patients with hand paralysis," *NeuroImage: Clin.*, vol. 14, pp. 726–733, 2017.
[31] R. Chaisaen, P. Autthasan, N. Mingchinda, P. Leelaarporn, N. Kunaseth, S. Tammajarung, P. Manoonpong, S. C. Mukhopadhyay, and T. Wilaiprasitporn, "Decoding EEG rhythms during action observation, motor imagery, and execution for standing and sitting," *IEEE Sensors J.*, early access, Jun. 30, 2020, doi: 10.1109/JSEN.2020.3005968.
[32] C. M. Stinear, "Prediction of motor recovery after stroke: Advances in biomarkers," *Lancet Neurol.*, vol. 16, no. 10, pp. 826–836, Oct. 2017.
[33] M. F. Folstein, S. E. Folstein, and P. R. McHugh, "'Mini-mental state': A practical method for grading the cognitive state of patients for the clinician," *J. Psychiatric Res.*, vol. 12, no. 3, pp. 189–198, 1975.
[34] C. Pacchierotti, S. Sinclair, M. Solazzi, A. Frisoli, V. Hayward, and D. Prattichizzo, "Wearable haptic systems for the fingertip and the hand: Taxonomy, review, and perspectives," *IEEE Trans. Haptics*, vol. 10, no. 4, pp. 580–600, Oct. 2017.
[35] T. Ball, A. Schreiber, B. Feige, M. Wagner, C. H. Lücking, and R. Kristeva-Feige, "The role of higher-order motor areas in voluntary movement as revealed by high-resolution EEG and fMRI," *NeuroImage*, vol. 10, no. 6, pp. 682–694, 1999.
[36] A. Y. Paek, H. A. Agashe, and J. L. Contreras-Vidal, "Decoding repetitive finger movements with brain activity acquired via non-invasive electroencephalography," *Frontiers Neuroeng.*, vol. 7, p. 3, Mar. 2014.
[37] N. Mizuguchi, H. Nakata, T. Hayashi, M. Sakamoto, T. Muraoka, Y. Uchida, and K. Kanosue, "Brain activity during motor imagery of an action with an object: A functional magnetic resonance imaging study," *Neurosci. Res.*, vol. 76, no. 3, pp. 150–155, Jul. 2013.
[38] Y. K. Kim, E. Park, A. Lee, C.-H. Im, and Y.-H. Kim, "Changes in network connectivity during motor imagery and execution," *PLoS ONE*, vol. 13, no. 1, Jan. 2018, Art. no. e0190715.
[39] M. Lee, J.-G. Yoon, and S.-W. Lee, "Predicting motor imagery performance from resting-state EEG using dynamic causal modeling," *Frontiers Hum. Neurosci.*, vol. 14, p. 321, Aug. 2020.
[40] J. Taylor, "Proprioception," in *Encyclopedia of Neuroscience*, L. R. Squire, Ed. Oxford, U.K.: Academic, 2009, pp. 1143–1149.
[41] S. Darvishi, A. Gharabaghi, C. B. Boulay, M. C. Ridding, D. Abbott, and M. Baumert, "Proprioceptive feedback facilitates motor imagery-related operant learning of sensorimotor β-band modulation," *Frontiers Neurosci.*, vol. 11, p. 60, Feb. 2017.
[42] R. C. Lyle, "A performance test for assessment of upper limb function," *Phys. Rehabil. Treatment Res.*, vol. 4, no. 4, pp. 483–492, 1981.
[43] M. Z. Baig, N. Aslam, H. P. H. Shum, and L. Zhang, "Differential evolution algorithm as a tool for optimal feature subset selection in motor imagery EEG," *Expert Syst. Appl.*, vol. 90, pp. 184–195, Dec. 2017.
[44] V. P. Oikonomou, K. Georgiadis, G. Liaros, S. Nikolopoulos, and I. Kompatsiaris, "A comparison study on EEG signal processing techniques using motor imagery EEG data," in *Proc. IEEE 30th Int. Symp. Computer-Based Med. Syst. (CBMS)*, Jun. 2017, pp. 781–786.
[45] S. Kumar, A. Sharma, and T. Tsunoda, "An improved discriminative filter bank selection approach for motor imagery EEG signal classification using mutual information," *BMC Bioinf.*, vol. 18, no. S16, p. 545, Dec. 2017.

[46] G. Pfurtscheller, T. Solis-Escalante, R. J. Barry, D. S. Klobassa, C. Neuper, and G. R. Müller-Putz, "Brisk heart rate and EEG changes during execution and withholding of cue-paced foot motor imagery," *Frontiers Hum. Neurosci.*, vol. 7, p. 379, 2013.
[47] A. Chowdhury, A. Dutta, and G. Prasad, "Can corticomuscular coupling be useful in designing hybrid-brain robot interfaces towards hand functional recovery?" in *Proc. IEEE Int. Conf. Syst., Man Cybern. (SMC)*, Oct. 2019, pp. 3619–3624.
[48] C. E. Lang, D. F. Edwards, R. L. Birkenmeier, and A. W. Dromerick, "Estimating minimal clinically important differences of upper-extremity measures early after stroke," *Arch. Phys. Med. Rehabil.*, vol. 89, no. 9, pp. 1693–1700, Sep. 2008.
[49] Y. Zheng, Y. Peng, G. Xu, L. Li, and J. Wang, "Using corticomuscular coherence to reflect function recovery of paretic upper limb after stroke: A case study," *Frontiers Neurol.*, vol. 8, p. 728, Jan. 2018.
[50] R. Krauth, J. Schwertner, S. Vogt, S. Lindquist, M. Sailer, A. Sickert, J. Lamprecht, S. Perdikis, T. Corbet, J. D. R. Millán, H. Hinrichs, H.-J. Heinze, and C. M. Sweeney-Reed, "Cortico-muscular coherence is reduced acutely post-stroke and increases bilaterally during motor recovery: A pilot study," *Frontiers Neurol.*, vol. 10, p. 126, Feb. 2019.
[51] C. Vidaurre and B. Blankertz, "Towards a cure for BCI illiteracy," *Brain Topography*, vol. 23, no. 2, pp. 194–198, Jun. 2010.
[52] G. Prasad, P. Herman, D. Coyle, S. McDonough, and J. Crosbie, "Applying a brain-computer interface to support motor imagery practice in people with stroke for upper limb recovery: A feasibility study," *J. Neuroeng. Rehabil.*, vol. 7, no. 1, p. 60, Dec. 2010.
[53] D. J. Hewson, J.-Y. Hogrel, Y. Langeron, and J. Duchêne, "Evolution in impedance at the electrode-skin interface of two types of surface EMG electrodes during long-term recordings," *J. Electromyogr. Kinesiol.*, vol. 13, no. 3, pp. 273–279, Jun. 2003.
[54] G. Naros, I. Naros, F. Grimm, U. Ziemann, and A. Gharabaghi, "Reinforcement learning of self-regulated sensorimotor β-oscillations improves motor performance," *NeuroImage*, vol. 134, pp. 142–152, Jul. 2016.
[55] J. L. Chen and G. Schlaug, "Increased resting state connectivity between ipsilesional motor cortex and contralesional premotor cortex after transcranial direct current stimulation with physical therapy," *Sci. Rep.*, vol. 6, no. 1, p. 23271, Mar. 2016.
[56] L. H. Larsen, I. C. Zibrandtsen, T. Wienecke, T. W. Kjaer, M. S. Christensen, J. B. Nielsen, and H. Langberg, "Corticomuscular coherence in the acute and subacute phase after stroke," *Clin. Neurophysiol.*, vol. 128, no. 11, pp. 2217–2226, Nov. 2017.
[57] H. E. Rossiter, C. Eaves, E. Davis, M.-H. Boudrias, C.-H. Park, S. Farmer, G. Barnes, V. Litvak, and N. S. Ward, "Changes in the location of cortico-muscular coherence following stroke," *NeuroImage: Clin.*, vol. 2, pp. 50–55, 2013.
[58] K. Wang, M. Xu, Y. Wang, S. Zhang, L. Chen, and D. Ming, "Enhance decoding of pre-movement EEG patterns for brain–computer interfaces," *J. Neural Eng.*, vol. 17, no. 1, Jan. 2020, Art. no. 016033.

ANIRBAN CHOWDHURY received the B.Tech. degree in electronics and communication engineering from the Kalyani Government Engineering College, India, the M.Tech. degree in mechatronics from the School of Mechatronics and Robotics, IIEST, Shibpur, India, and the Ph.D. degree in mechatronics from the Centre for Mechatronics, IIT Kanpur, India. He was a Postdoctoral Research Associate with the Northern Ireland Functional Brain Mapping Facility, Ulster University, Northern Ireland, U.K. He has contributed to two U.K.–India thematic partnership projects funded by the British Council, U.K., and the Department of Science and Technology. India. He has also led the successful completion of two clinical trials on post-stroke robot-assisted neurorehabilitation, one in India and the other in U.K. He is currently a Lecturer in Computer Science and Artificial Intelligence with the School of Computer Science and Electronic Engineering (CSEE), University of Essex (UoE), and a member of BCI-NE and the Robotics Group, UoE. His current research interests include robotic rehabilitation, brain–computer interfaces, assistive technologies, human–robot co-operation, and autonomous mobile robotics.

ASHISH DUTTA (Member, IEEE) received the Ph.D. degree in systems engineering from Akita University, Akita, Japan.

From 1994 to 2000, he was with the Bhabha Atomic Research Center, Mumbai, India, where he researched telemanipulator design and control for nuclear applications. Since 2002, he has been with the Department of Mechanical Engineering, Indian Institute of Technology Kanpur, Kanpur, India. He was also a Visiting Professor with Nagoya University, Nagoya, Japan, in 2006. He is currently a Visiting Professor with the Kyushu Institute of Technology, Kitakyushu, Japan. His current research interests include bio-robotics, robot–human interaction, intelligent control systems, and rehabilitation engineering.

GIRIJESH PRASAD (Senior Member, IEEE) received the B.Tech. degree in electrical engineering, the M.Tech. degree in computer science and technology, and the Ph.D. degree in electrical engineering from Queen's University, Belfast, U.K., in 1987, 1992, and 1997, respectively.

He currently holds the post of Professor of Intelligent Systems with the School of Computing, Engineering and Intelligent Systems, Ulster University, Magee campus. As an Executive Member of the Intelligent Systems Research Centre, Magee campus, he also leads the Neural Systems and Neurotechnology Team. He is also the Director of the Northern Ireland Functional Brain Mapping facility for MEG studies. His research interests include computational intelligence, brain modeling, brain–computer interfaces and neuro-rehabilitation, and assistive robotic systems. He has published more than 230 research papers in international journals, books, and conference proceedings. He is a Chartered Engineer and a Fellow of the IET and the International Academy of Physical Sciences. He is a Founder Member of IEEE SMC TCs on Brain–Machine Interface Systems.